TOWARDS MANUFACTURING AND METROLOGY OF ROLL-TO-ROLL HOLOGRAPHIC NANOSTRUCTURES

Luis Arturo Aguirre[1], Barbara Groh[1], Kwon Sang Lee[1], Shashank Venkatesan[2], Liam G. Connolly[3], Michael Baldea[2], Chih-Hao Chang[1], and Michael Cullinan[1]
[1]Walker Department of Mechanical Engineering
University of Texas at Austin
[2]McKetta Department of Chemical Engineering
University of Texas at Austin
[3]Microsystems and Nanotechnology Division, Physical Measurement Laboratory
National Institute of Standards and Technology

INTRODUCTION

3D nanoscale manufacturing historically requires precise overlay alignment to ensure inter-layer connection. Due to the instability of the web in roll-to-roll (R2R) manufacturing, multilayer alignment remains a significant challenge to overcome before it can compete with solid-substrate manufacturing at the nano scale.

A solution to the multilayer alignment challenge in R2R is to leverage interference lithography to cure 3D holographic structures to cure the full 3D pattern in a single exposure. This eliminates the need for overlay alignment and allows high-throughput manufacturing to further expedite the R2R manufacturing process. To achieve the nanometer level registration, a deterministic approach using the principles of precision engineering is required. This is critical due to the flexibility of the mask and the subtrate that cannot suffer deformation or be subject to changing tension. In addition, 3D manufacturing introduces the need for 3D metrology. Volumetric light based methods such as scatterometry will give insight into the average pattern-level success. Feature-scale surface metrology with AFM will provide insight into local defects that are indicative of failures within the pattern such as holes or inernal collapses.

MAJOR TOOL MODULES

The full system leverages a series of manufacturing and metrology modules in an effort to build a machine capable of real-time process control. A simplified image of the system is shown in Fig.1. The main machine sections consist of the lithography module, the wet processing and development module, and the metrology module. Each of these consists of further sub-systems crucial to its operation. The web moves continuously between modules on rollers with precision sin-cos encoders and load cells for tension monitoring. The functions of the lithography module are explained further in their corresponding section, with focus on the lithography and metrology modules.

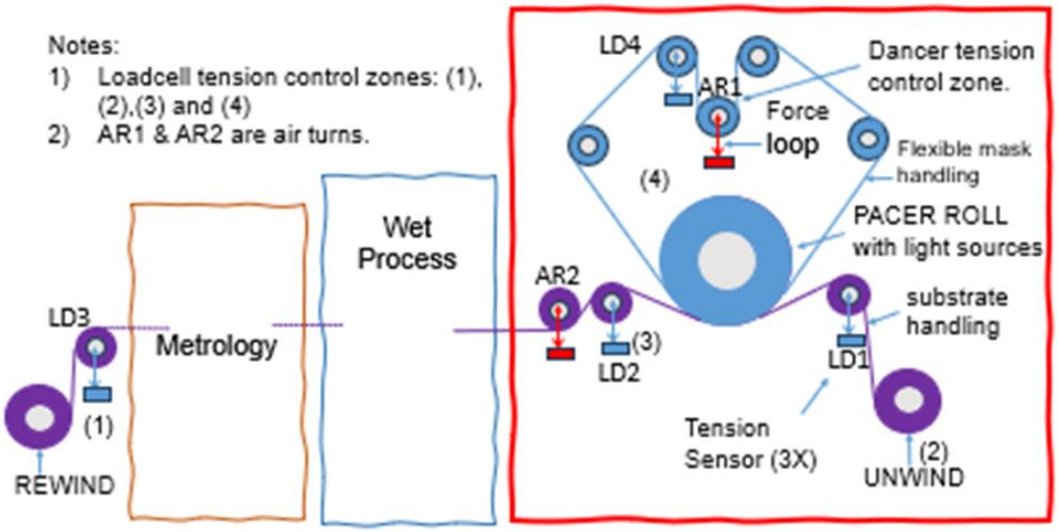

Figure 1 Diagram of planned manufacturing system

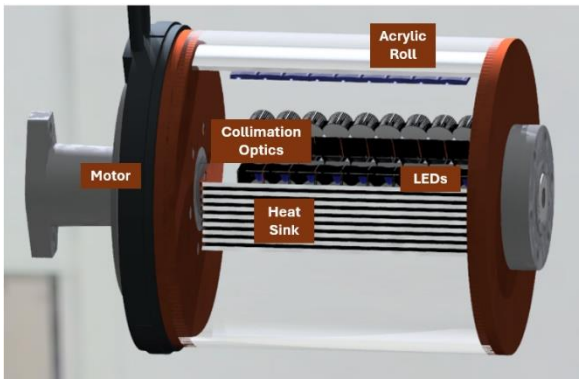

Figure 3. Pacer model including 9/each 365 nm LEDs sources and required optics.

LITHOGRAPHY MODULE

The lithography module consists of two interacting webs. The first is the diffractive optic mask web [1], indicated by the rollers IR2, IR3, IR4, LD2, AR1 and pacer roll in Fig. 1. This web drives the interaction between the mask and the substrate, both bringing the mask into contact and controlling the exposure. It also ensures that the mask web moves at the same speed as the second web in the system, the substrate web. The substrate webline proceeds through the rest of the modules, but within the lithography module, it is driven and held up to the exposure area by the virtual NIP, created by two tension rollers around the pacer as illustrated in figure 1. For developing subwavelength holographic deep structures on the resist, the 3D mask and the resist films need to be in contact – due to the near field requirements [2], with very low pressure to avoid deformation of the mask cavities and the resist thickness.

Lithography Pacer

The lithography pacer roller is the heart of the lithography module. It is a unique innovation that contains the light sources and lenses that allow for the mask and substrate to be exposed. Its major components are shown in Fig. 2, currently only showing the nine 365 nm LEDs within the system. For deep exposure of two wavelengths (365 nm and 405 nm), we use the irradiance of 50 mJ/cm2 along the films contact band with light collimated +/-2.5 deg over the whole exposure area. This is a difficult task considering that the two wavelengths are designed with space constraints residing inside a UVT acrylic 150 mm diameter cylinder. Given the limited space, this is achieved with a simplified optical design based on AL offset parabolic AL reflectors and surface mounted LEDs.

The controls for high performance nanometer registration are based on direct drive air bearing rollers, high resolution encoders and low noise tension loadcells integrated with high performance motion controller using cascade loops to trim the velocity and maintain the phase allowing around 100 nm registration and minimum film deformations[3].

LITHOGRAPHY MODULE

The lithography roll and its interaction with the webline is the central operation within the lithography module. Its functionality is directly related to the quality of the exposure and the precision of the webline motion. Therefore, two major modeling and testing thrusts have emerged.

Exposure Simulations and model verification

As the lithography module exposure is driven by an LED array, it is critical that the exposure dosage and power density of the LED are modeled to ensure even exposure. A ray trace analysis and luminosity distribution model demonstrate that maintaining collimation within 5% of the desired angle of incidence can result in curing variations up to 13% [4]. To test the vendor-supplied ray file, we measured the LED by projecting to a beam profiler located at 20, 30 and 40 mm, using an ND filter to protect the beam profiler. Given that the beam was larger than our beam profiler, we acquired 36 images with overlap to build a full frame 36x24 mm image as illustrated in figure 3.

To validate the ray file, we used the output mesh of the simulation using Synopsis LightTools© as shown in figure 4 and compared with the outputs from the real LED as shown in figure 5.

The results of the gaussian fit show that the actual beam is very close to the simulated one.

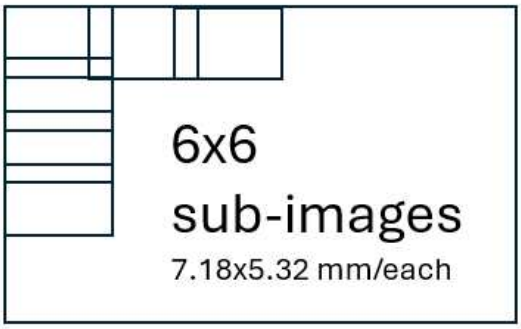

Figure 2: Our beam profiler Ophir Model SP928 with the size 7.18x5.32 mm X 36 created the 34x24 image.

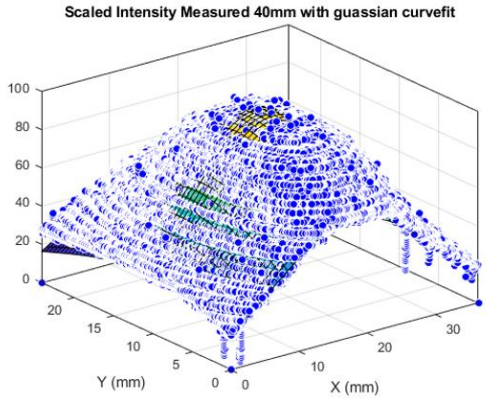


```
Measured mesh at 40 mm:
     General model:
     val(x,y) = a*exp(-((x-b).^2 + (y-c).^2)/d)
     Coefficients (with 95% confidence bounds):
       a =        96.9  (96.9, 96.9)
       b =       17.92  (17.92, 17.92)
       c =       11.18  (11.18, 11.18)
       d =       274.1  (274.1, 274.2)
```

Figure 5: Mesh created using the vendor supplied ray file and our simulation tool.

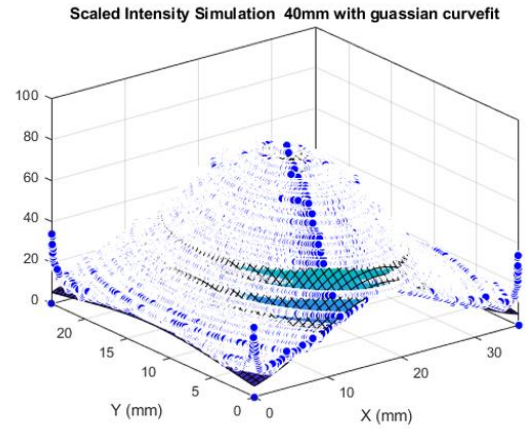


```
Measured mesh at 40 mm:
     General model:
     val(x,y) = a*exp(-((x-b).^2 + (y-c).^2)/d)
     Coefficients (with 95% confidence bounds):
       a =       80.47  (80.45, 80.49)
       b =       17.98  (17.97, 17.98)
       c =       11.98  (11.97, 11.98)
       d =       173.2  (173.1, 173.2)
```

Figure 4: Mesh created scanning the sensor to create the mesh.

Webline Simulation and prototype results

Due to the length of the webline and its inherent interactions with multiple manufacturing and processing modules within this interlinked manufacturing process, maintaining precision webline motion is critical to the success of the project. As such, extreme care must be taken to maintain exact constraint of the system and the following architecture is considered to eliminate over constraint.

Firstly, web motion will be primarily driven by the Pacer and followed by the unwind with the Mask film sandwiched in between. In here, the substrate tension will be regulated by changing the speed of the unwind roller as it is illustrated in figure 7. On the other end, The Metrology roller that also needs the same tension as above, the rewind roller speed will be regulated using the same approach. By leveraging flexible rollers in between precision rollers with a single-DOF, each module in a system can be treated separately. For example, the interaction between the pacer and the unwind is not over constrained since the tension roll is flexible. In addition, this allows the lithography pacer and AFM stabilizing idler roller to each be mechanically independent. The connection in between is dictated by using the pacer linear position that is used in both as a position reference. The key of the design is to achieve minimum constraints over the overall machine, especially when the rollers are close to each other by using flexible mounts, air turns and gimballed rollers.

The tension rollers are designed with unique cylindrical flexures shown in figure 6 that allow a lower vertical and lateral stiffness and only act as support and tension sensor. With the tension rollers, we have been able to achieve a 0.05 gr-force resolution by measuring the deflection with a capacitance gage.

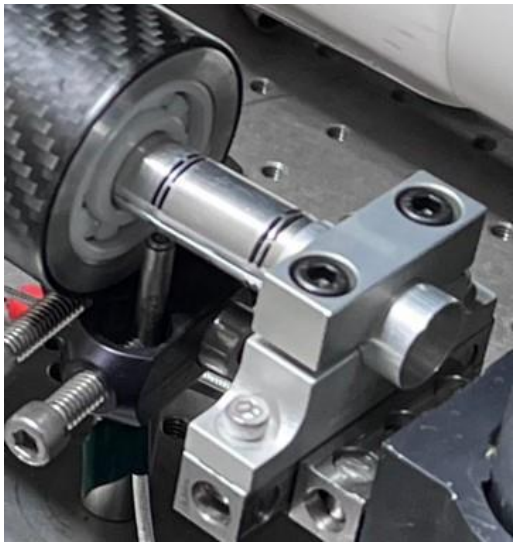

Figure 6. One side tension roller custom flexure of rolled aluminum.

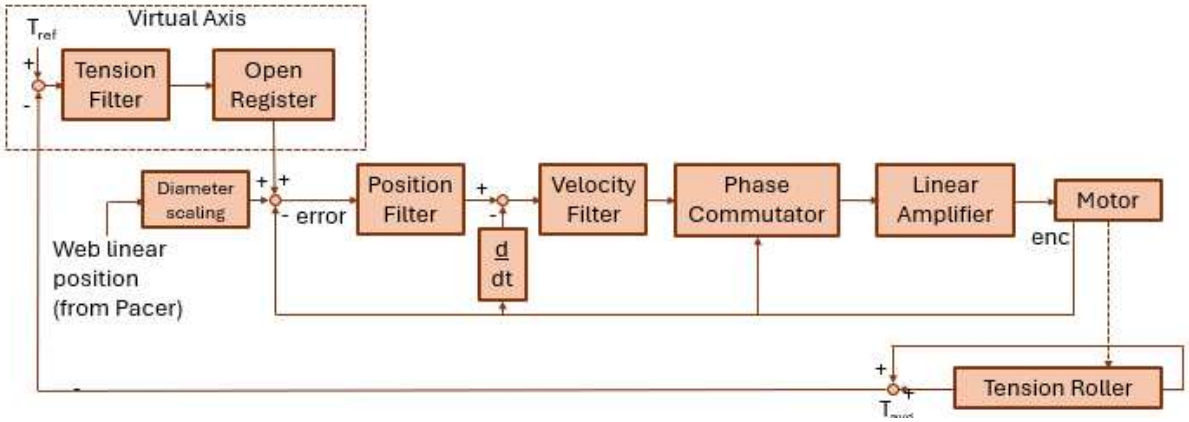

Figure 7. Typical Tension Control Loop

To reduce static friction and the roller mass, we implemented the prototype using ceramic bearings and carbon fiber sleeve. With that resolution as feedback the velocity of the unwind and rewind motors can be controlled to maintain both the desired web speed and the required web tension on the areas that are critical. In addition, they provide the proper flexibility, minimizing any web deformations.

METROLOGY MODULE

Since both feature scale sub-diffraction metrology and larger pattern-scale metrology are necessary to fully characterize the final defect detection to indicate issues with the mask or development processes. Metrology is critical in precision manufacturing as feedback control to create an optimized system.

Web-Scale Metrology

The scatterometry module conducts larger scale optical characterization using both experimental reflectance spectra and analytical models. The analytical models provide a baseline comparison to pre-generated structures to provide a baseline for volumetric characterization [6].

MACHINE LEARNING PROCESS CONTROL

The ultimate goal of in-line metrology within this R2R manufacturing system would be to provide real-time feedback control to the manufacturing process. However, due to the high computational load of both AFM and scatterometry metrology, further innovation is necessary before these sources can be reliable for real-time control. Specifically, building a metrology database and machine learning algorithm focused on combining the data from the multimodal sources and delivering the results to algorithms targeted towards defect detection and feature characterization.

CONCLUSIONS:

Precision webline manufacturing using flexible mask film presents a unique challenge or opportuity to use precision engineering principles. In addition, besides nanometer registration, given the soft Mask with 3D features, low tension control required to expose and inspect the substrate. In addition, precision engineering principles has given us the tools that we need to decoupled and utilize exact constraint [3] to minimize mask and substrate deformations. We expect that this deterministic approach will simplify the integration and help address the sources of errors so appropiately.

SOURCES

[1] P. Pandya, “Roll-to-Roll Nanoimprint Lithography with Sub-50 nm Features and Sub-25 nm Residual Layer Thicknesses,” Boston, MA, Nov. 20, 2023.

[2] I.-T. Chen, “Large-Scale Manufacturing of Three-Dimensional Periodic Nanostructures and Their Applications,” Dissertation, University of Texas at Austin.

[3] D. Blanding, “Exact Constraint: Machine Design Using Kinematic Principles,” *ASME Press*, 1997.

[4] B. Groh, K. S. Lee, L. A. Aguirre, and M. Cullinan, “Manufacturing and metrology of 3D holographic structure nanopatterns in roll-to-roll fabrication,” *SPIE*, vol. 12956, Apr. 2024, doi: https://doi.org/10.1117/12.3010004.

[5] L. G. Connolly, T.-F. Yao, A. Chang, and M. Cullinan, “A tip-based metrology framework for real-time process feedback of roll-to-roll fabricated nanopatterned structures,” *Precision Engineering*, vol. 57, pp. 137–148,

May 2019, doi: 10.1016/j.precisioneng.2019.04.001.
[6] K. S. Lee, K.-C. Chien, B. Groh, I.-T. Chen, M. Cullinan, and C.-H. Chang, “Characterization of porosity in periodic 3D nanostructures using spectroscopic scatterometry,” *Journal of Vacuum Science & Technology B*, vol. 41, no. 6, p. 064001, Dec. 2023, doi: 10.1116/6.0003035.